JOURNAL OF CATALYSIS 110, 139–149 (1988)

X-Ray Photoelectron and Ion Scattering Studies of Tungsten Oxides and Tungsten Oxide Catalysts

P. J. C. CHAPPELL,[1] M. H. KIBEL,[2] AND B. G. BAKER

School of Physical Sciences, The Flinders University of South Australia, Bedford Park, South Australia 5042, Australia

Received August 19, 1986; revised October 6, 1987

X-ray photoelectron spectroscopy and ion scattering spectroscopy are employed to study well-defined mixed valence oxides of tungsten and an operational alkene isomerisation catalyst, consisting of alumina-supported tungsten trioxide which is partially reduced by preconditioning in hydrogen saturated in water vapour. Both γ-alumina and γ-alumina partially transformed to α-alumina by heating are used as catalyst supports. In both cases it is found that the tungsten trioxide interacts with the alumina to form an irreducible surface species in which the tungsten is tetrahedrally coordinated. Sodium impurities in the alumina appear to assist the reaction. Catalysis takes place on the partially reduced tungsten oxide species which is stabilised by a weak interaction with the alumina. The heat-treated alumina is a better catalyst support because, for equivalent loadings, its smaller surface area leaves more free tungsten trioxide for reduction and subsequent catalytic activity.

INTRODUCTION

There are many examples in the literature which indicate that X-ray photoelectron spectroscopy (XPS) is an excellent technique for distinguishing changes in the oxidation state of transition metals (*1–5*). Furthermore, XPS can provide such information even when a metal oxide is supported on a substrate such as silica or alumina. In the present study, we have used XPS, together with ion scattering spectroscopy (ISS), to investigate various unsupported and supported tungsten oxides. This study has been undertaken in an attempt to understand how such compounds function as catalysts. In particular we are interested in their application as isomerisation catalysts following the Fischer–Tropsch (F–T) process.

Catalysts currently being used for F–T synthesis produce predominantly straight-chain hydrocarbons. For many industrial applications, however, branched chains are desirable. In the production of gasoline, for example, branched-chain hydrocarbons are preferred because of their higher octane rating. An isomerisation catalyst is necessary to achieve this outcome. A new catalyst has recently been developed (*6, 7*) to isomerise straight-chain alkenes produced in the F–T process to branched alkenes. This catalyst consists of alumina-supported tungsten trioxide (WO_3) which has been partially reduced by preconditioning in hydrogen saturated with water vapour. WO_3 is well known as a metathesis catalyst (*8–12*), but its application to alkene isomerisation, although previously noted (*12, 13*), has attracted little attention.

We have employed XPS in an attempt to detect the changes which occur on the isomerisation catalyst during its conditioning and operation in the gas stream. This has involved a study of both unsupported and supported oxides, in order to determine the nature of any tungsten–support interaction. In addition ISS, which is probably the most surface-sensitive spectroscopic tech-

[1] Present address: Materials Research Laboratories, P.O. Box 50, Ascot Vale, VIC 3032, Australia.

[2] To whom correspondence should be addressed at Telecom Australia Research Laboratories, 770 Blackburn Road, Clayton, VIC 3168, Australia.

0021-9517/88 $3.00

nique presently available, has been used to examine the actual surface of these compounds.

METHODS

(a) *Instrumentation*

The experiments described below were performed on a Leybold–Heraeus LHS-10 surface analysis system. The main chamber is evacuated by a 450 Ls^{-1} turbomolecular pump and a titanium sublimation pump, which routinely achieve a base pressure of 10^{-10} mbar. This instrument is equipped for X-ray and ultraviolet photoelectron spectroscopy (XPS and UPS), Auger electron spectroscopy (AES), and ion scattering spectroscopy (ISS) and has a quadrupole mass spectrometer for residual gas analysis. There is also an electron flood gun (tungsten wire filament) which produces a beam of low-energy electrons to neutralise sample charging. The sample is mounted on a stainless-steel rod constructed to allow sample heating, the temperature being monitored by a chromel–constantan thermocouple. From atmosphere the rod is loaded through a vacuum introduction lock into a preparation chamber separated from the main chamber by a gate valve. The preparation chamber is separately pumped by a 220 Ls^{-1} turbomolecular pump, allowing samples to be transferred directly from reaction conditions to vacuum for analysis.

The heart of this surface analysis system is a conventional hemispherical electrostatic analyser, combined with a retarding lens and an off-axis entrance slit, which provides excellent resolution. The X-ray photoelectron spectra recorded in this work were obtained with Mg$K\alpha$ radiation (1253.6 eV), which has a linewidth of 0.8 eV. (For XPS the resolution is limited by the natural linewidth of the X-ray source.) The spectrometer was calibrated using the 4*f* peaks of gold. Sample charging was not found to be a problem for the unsupported oxides, because they are semiconductors. The supported oxides all exhibited some sample charging, usually a few electron volts. The flood gun was used to confirm sample charging, and the Al 2*p* peak of Al_2O_3 was used as a reference to calculate the shift due to charging.

For the present spectra the analyser was run in fixed analyser transmission (FAT) mode, i.e., constant pass energy (ΔE), with no discrimination against low-energy electrons. A pass energy of 20 eV was found to give optimum resolution with acceptable intensity. The polarity of the analyser and detector can be reversed in order to detect ions rather than electrons, thus allowing ion scattering spectra to be obtained. In this case the analyser was run in fixed retardation ratio (FRR) mode; i.e., ($\Delta E/E$) is constant, where E is the photoelectron energy. The ion scattering spectra recorded in this work were obtained with $\Delta E/E = 3$. Both XPS and ISS data were collected and stored via a 12-bit A/D converter and a Commodore Pet 4016 microcomputer.

(b) *Preparative Method*

Tungsten trioxide (WO_3) and aluminium tungstate ($Al_2(WO_4)_3$) were obtained commercially as powders. The substoichiometric oxides $WO_{2.9}$ ($W_{20}O_{58}$) and $WO_{2.72}$ ($W_{18}O_{49}$) were obtained by heating stoichiometric quantities of W and WO_3 powders in a sealed evacuated quartz tube for 1 week. X-ray powder diffraction patterns were used to confirm the identity of the products. The tungsten dioxide (WO_2) sample was produced by reducing a pellet of WO_3 in wet hydrogen ($pH_2/pH_2O \simeq 40$) at 405°C for 15 h. The reduction process was followed by monitoring the W 4*f* peaks by XPS, with the resultant spectra being shown in Fig. 1. Although this sample is not pure (there is still some higher oxide present and also a small amount of metal) the sample had the brown colour expected for WO_2, and the W 4*f* peaks have well-defined positions distinct from those of the other oxides in this study.

The supported WO_3 catalysts were routinely prepared by impregnation of the support with aqueous sodium tungstate solu-

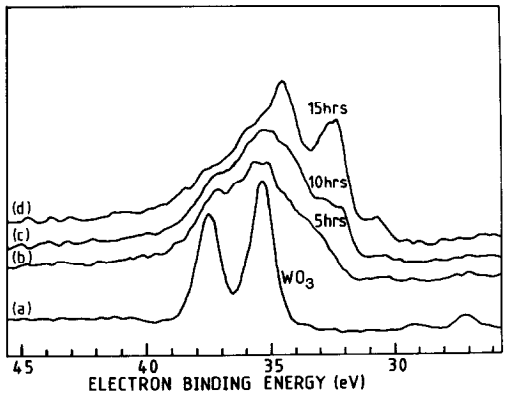

FIG. 1. XP spectra of unsupported WO_3 reduced in wet hydrogen (pH_2/pH_2O = 40) at 405°C. (a) WO_3 before reduction; (b) after 5 h reduction; (c) after 10 h reduction; (d) after 15 h reduction.

tion followed by treatment to form tungstic acid and dehydration to form tungsten trioxide. The exact preparative details have been given previously (*6, 7*). In the present work all supported samples had a loading of 6% by weight of WO_3.

(*c*) *Experimental Method*

All of the powdered samples were pressed into small stainless-steel cups to a pressure of 11 MPa in order to form pellets and were then cleaved in atmosphere level with the top of the cup. This procedure minimised contamination from the pellet press. The pellets were then clamped onto the sample rod and passed through the vacuum lock into the preparation chamber. Sample reduction was achieved by heating the sample in flowing hydrogen which had been passed through either a molecular sieve trap or water to dry or wet the hydrogen. At the conclusion of the hydrogen treatment the rod was cooled, the hydrogen was evacuated from the preparation chamber, and the sample was transferred directly into the main chamber for analysis.

RESULTS

(*a*) *Unsupported Tungsten Oxides*

Presented in Fig. 2 are the W 4*f* spectra of tungsten metal and the four common oxides. These spectra are similar to those reported by de Angelis and Schiavello (*1*), except for WO_2, for which they reported higher binding energies for W than those indicated by the present study. This may reflect different methods of preparation; our sample was reduced from WO_3 *in situ*, while de Angelis and Schiavello used commercial WO_2 powder. It is possible that the surface of their powdered sample was oxidised, thereby giving rise to higher W 4*f* binding energies.

While it is accepted that WO_3 and WO_2 contain only W^{6+} and W^{4+} oxidation states, respectively, the contributions to the stoichiometry of $W_{18}O_{49}$ and $W_{20}O_{58}$ are not as unambiguous. For example, Fig. 3 represents an attempt to model the spectrum of $W_{20}O_{58}$ assuming contributions from discrete W^{6+} and W^{5+} ions only, in the ratio 16:4. For this procedure our spectrum of WO_3 was used as the definitive spectrum of

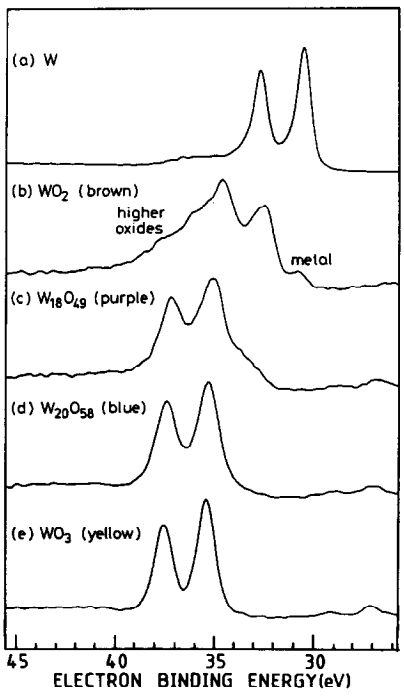

FIG. 2. W 4*f* XP spectra of tungsten and four unsupported tungsten oxides. (a) W powder; (b) WO_2; (c) $W_{18}O_{49}$; (d) $W_{20}O_{58}$; (e) WO_3.

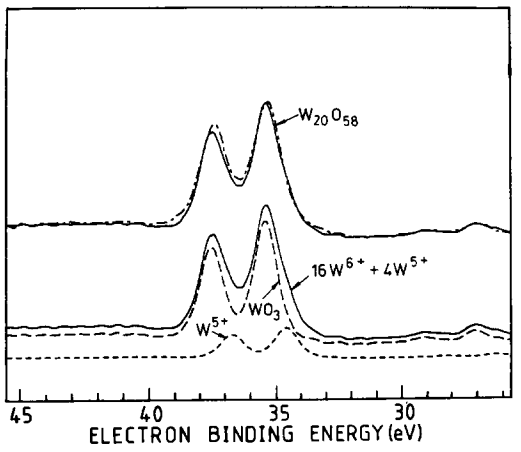

FIG. 3. Attempt to fit the $W_{20}O_{58}$ spectrum from $W_{16}^{6+}W_4^{5+}$ using the WO_3 spectrum as a model. (---) W^{5+}; (—·—) W^{6+}; (—) $16W^{6+} + 4W^{5+}$; (---) $W_{20}O_{58}$ (experimental).

W^{6+}. The W^{5+} component was then assumed to be identical to the W^{6+}, but displaced by an amount equivalent to one unit of charge, i.e., one-sixth of the shift between W^{6+} and W^0.

The spectrum of $W_{18}O_{49}$ is the most complicated of the tungsten oxide spectra. In practice it was not possible to fit the recorded spectrum to any of the integral stoichiometric combinations of W^{6+}, W^{5+}, and W^{4+}. The problems associated with $W_{18}O_{49}$ are discussed in more detail later.

(b) *Supported Tungsten Oxides*

The results for supported tungsten oxides are shown in Figs. 4–8 and are summarised in Table 1.

Figure 4 shows the effect of heating a sample of 6% WO_3/γ-Al_2O_3 in air. There is virtually no change in the W 4*f* spectrum below about 400°C (see spectra (a) and (b)). However, after heating for only 1.5 h at 400°C there is an obvious shift to higher binding energy (spectrum (c)), implying a change in the chemical environment of the tungsten. After 20 h at 400°C this change is virtually complete and, as can be seen by comparison with spectrum (e), the resultant spectrum (d) is almost identical to that for $Al_2(WO_4)_3$. A subsequent attempt to reduce this catalyst in wet hydrogen was unsuccessful, as shown in Fig. 5a. Further treatment in dry hydrogen resulted in about 15%

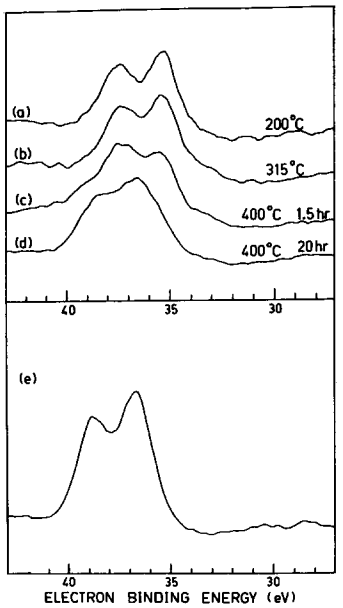

FIG. 4. XP spectra of a sample of 6% WO_3/γ-Al_2O_3 heated in air. (a) Heating to 200°C; (b) heating to 315°C; (c) heating at 400°C for 1.5 h; (d) heating at 400°C for 20 h; (e) XP spectrum of $Al_2(WO_4)_3$.

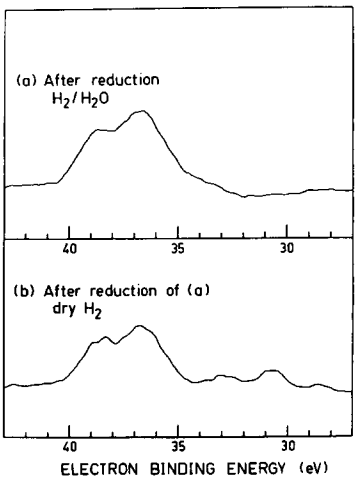

FIG. 5. XP spectra of sample from Fig. 4d after the following treatment. (a) Exposure to wet hydrogen at 400°C. (b) Subsequent exposure to dry hydrogen at 400°C (15% reduction).

TABLE 1

XPS Results for Supported Catalysts

Sample (all 6% loadings)	W $4f_{7/2}$ binding energy (eV) for WO_x				Percentage reduction total	Figure no.
	As loaded	Calcined in air	Wet H_2(400°C)	Dry H_2(400°C)		
WO_3/γ-Al_2O_3	35.2	36.7(400°C)	36.7	36.7	15	4,5
WO_3/γ-Al_2O_3	35.2	35.2(200°C)	—	—[a]	75	6
WO_3/HT-Al_2O_3	35.6[b]	—	35.6 34.9[c]	35.4	30	8
WO_3/washed HT-Al_2O_3	37.0[b]	—	36.7	36.1	41	—
WO_3/HT-Al_2O_3	35.6	36.3(450°C)	—	—	—	7

[a] Insufficient WO_x remained unreduced to enable a binding energy to be determined.
[b] Very broad, overlapping peaks.
[c] Intermediate state, determined by spectrum subtraction (see Fig. 8 and text).

of the supported oxide being reduced to tungsten metal (Fig. 5b).

Figure 6 represents another sample of the 6% WO_3/γ-Al_2O_3 catalyst heated to only 200°C in air and then subsequently treated with dry hydrogen. This treatment resulted in 75% of the supported oxide being reduced to tungsten metal (Fig. 6b).

It is well known (*14, 15*) that if γ-Al_2O_3, which contains both octahedrally and tetrahedrally coordinated Al, is calcined in air at high temperatures (>1000°C) it is converted to a corundum structure, commonly known as α-Al_2O_3, in which all of the Al is octahedrally coordinated. In our laboratory we have used γ-Al_2O_3 which has been heat-treated at 1250°C for a brief time (typically 10–15 min). The resultant alumina, which we call "heat-treated" or HT-alumina, is similar to α-Al_2O_3 but is slightly different in structure. It is more basic than γ-Al_2O_3 and has a surface area of ~15–20 $m^2\ g^{-1}$, com-

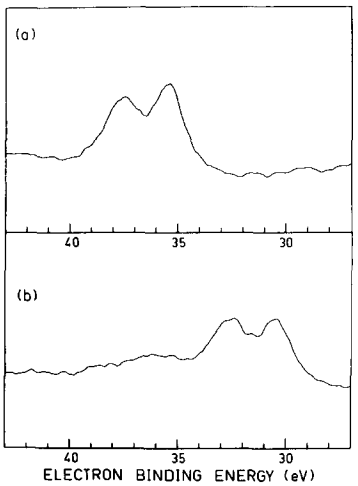

FIG. 6. XP spectra of a 6% WO_3/γ-Al_2O_3 sample. (a) Heated in air to only 200°C. (b) Subsequent exposure to dry hydrogen at 400°C (75% reduction).

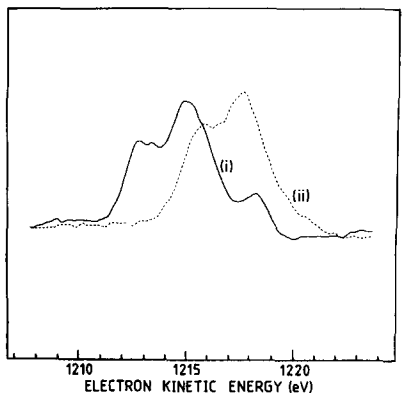

FIG. 7. A sample of unreduced WO_3/HT-Al_2O_3 (air, 450°C) serves as an example of how charging by X-rays can complicate a spectrum. (i) Spectrum recorded without using the flood gun. (ii) Flood gun used to discharge sample; 2.7 eV charge (see text).

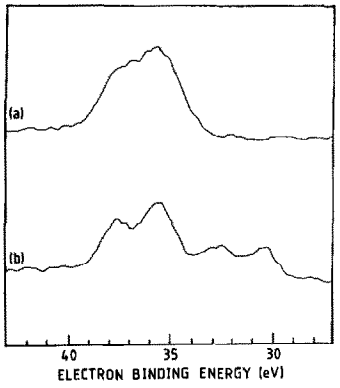

FIG. 8. XP spectra of a 6% WO_3/HT-Al_2O_3 sample. (a) After exposure to wet hydrogen at 400°C. (b) After subsequent dry hydrogen treatment at 400°C (30% reduction).

pared to 78 $m^2\ g^{-1}$ for γ-Al_2O_3 and generally $<1\ m^2\ g^{-1}$ for α-Al_2O_3. The HT-Al_2O_3 has been found to be far superior to γ-Al_2O_3 when used as a support for catalysts in this laboratory (*6*).

When 6% WO_3/HT-Al_2O_3 is heated in air above 400°C the resultant W 4*f* spectrum (Fig. 7(i)) is different from that of 6% WO_3/γ-Al_2O_3 treated similarly (Fig. 4). The presence of three peaks in the W 4*f* spectrum of the HT-Al_2O_3-supported oxide is explained by incomplete sample charging. When the flood gun is used to compensate for the loss of electrons, the spectrum collapses to two peaks (Fig. 7(ii)). The small peak at high kinetic energy in the uncompensated spectrum is due to uncharged WO_3, while the other two peaks arise from charged WO_3 which has presumably undergone some reaction with the HT-Al_2O_3, as in the case of γ-Al_2O_3. The smaller component of the uncharged WO_3 peak is overlapped by the larger charged component. From the spectrum the amount of charged material may be estimated to be about 25% of the total WO_3. Upon treatment in dry hydrogen the uncharged material was all reduced to metal. It should be noted that for both γ-Al_2O_3- and HT-Al_2O_3-supported catalysts only a single (charged) Al 2*p* peak is observed. It is for this reason that the Al 2*p* peak is used to monitor charging.

If the 6% WO_3/HT-Al_2O_3 sample is treated in wet hydrogen instead of air, the spectrum is somewhat different (Fig. 8a). Here, the spectrum is quite broad, but has no uncharged component. Treatment of this sample in dry hydrogen (Fig. 8b) resulted in 30% of the WO_3 being reduced to the metal.

In order to clarify the nature of the surface species present on the WO_3/HT-Al_2O_3 catalysts, we have used ion scattering spectroscopy. Figure 9 shows He^+ ion scattering spectra for bulk WO_3 and HT-Al_2O_3 for reference, as well as those for both heated and unheated 6% WO_3/HT-Al_2O_3 and for bulk $Al_2(WO_4)_3$. Note from curves (c) and (d) the increased intensity of the W peak for the heated catalyst. However, both of these spectra are different from spectrum (e), that of bulk $Al_2(WO_4)_3$. These results are presented in Table 2 in the form of peak intensities. The relationship between these

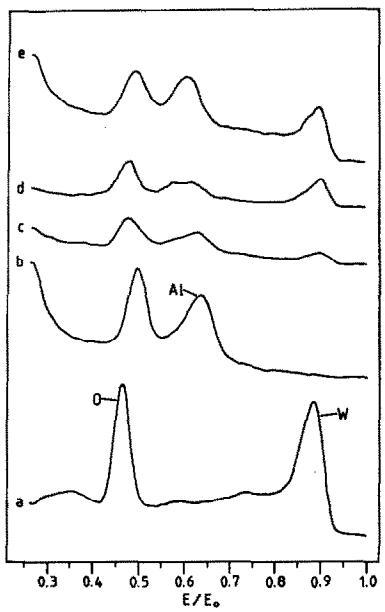

FIG. 9. He^+ (E_0 = 1 kV) ion scattering spectra of (a) bulk WO_3; (b) HT-Al_2O_3; (c) 6% WO_3/HT-Al_2O_3, untreated; (d) 6% WO_3/HT-Al_2O_3, heated in air at 400°C for 20 h; (e) bulk $Al_2(WO_4)_3$. Note that the slight variations in peak positions between spectra are due to sample charging.

TABLE 2

ISS Results for Supported Catalysts

Sample	Treatment	Intensity[a]		Curve in Fig. 9
		Al	W	
6% WO_3/HT-Al_2O_3	None	0.63	0.36	c
6% WO_3/washed HT-Al_2O_3	None	0.66	0.37	—
6% WO_3/washed HT-Al_2O_3	Reduced in H_2/H_2O, 2 h at 400°C	0.65	0.47	—
6% WO_3/washed HT-Al_2O_3	Reduced in H_2/H_2O, 2 h at 400°C, then H_2, 2 h at 400°C	0.81	0.62	—
6% WO_3/HT-Al_2O_3	Heated in air, 20 h at 400°C, reduced H_2/H_2O, then H_2 at 400°C	0.27	1.15[b]	d
$Al_2(WO_4)_3$	None	1.02	1.11[b]	e

[a] Intensities normalized to O peak.
[b] W : O intensity ratios similar.

results and the XPS data is investigated in the following discussion section.

DISCUSSION

(a) *Unsupported Tungsten Oxides*

The spectra of the tungsten oxides shown in Fig. 2 indicate that the binding energy, or chemical shift, of the W 4*f* peaks varies monotonically with oxidation state, from W^{6+} in WO_3 to W^0 in the metal. The interpretation of the $W_{20}O_{58}$ spectrum is straightforward. $W_{20}O_{58}$ has a structure which is related to that of WO_3 in that it has predominantly corner-shared octahedral WO_6 units with shear planes generated by edge sharing of octahedra to accommodate the oxygen deficiency (*16, 17*). $W_{20}O_{58}$ is the best known of a number of such oxides (*18*). A good fit to the W 4*f* peaks in this oxide has been obtained by assuming that the tungsten is divided between W^{6+} and W^{5+} in the ratio 16 : 4, where the position of W^{5+} is linearly interpolated between W^{6+} and W^0.

Accounting for the WO_2 and $W_{18}O_{49}$ spectra is more difficult. On the basis of a linear relationship between charges on the tungsten and chemical shift, one would expect the W $4f_{7/2}$ peak in WO_2 to have a binding energy of 33.7 eV. However, in our spectrum the peak appears at 32.4 eV. The reason for this apparent anomaly lies in the structure of WO_2, which is a distorted rutile structure. The tungsten atoms are not equally spaced, but rather form a network with alternating W–W distances of 2.50 and 3.14 Å (*19*). The tungsten atoms separated by only 2.50 Å are sufficiently close to form a bond. Thus, each tungsten atom gains electron density and the binding energy is reduced.

The structure of $W_{18}O_{49}$ has elements of the structure of both WO_3 and WO_2. It is an irregular structure with both edge and corner sharing of distorted octahedra, with hexagonal channels running through it (*20*). We have already noted that the W 4*f* spectrum of this oxide cannot be expressed as a combination of integral amounts of W^{6+}, W^{5+}, and W^{4+} if a linear relationship between charge and chemical shift is assumed. Because chemical shift is determined by electron density around the atom in question, it is interesting to examine the structure of the oxide to see if distinct oxidation numbers can be assigned to the individual tungsten atoms in the unit cell. A full

calculation involving molecular orbital theory is not feasible, but a first-order approximation can be obtained by considering the disposition of oxygen atoms in the unit cell. Despite the irregular structure, each tungsten atom is coordinated to a distorted octahedron of oxygen atoms. Each oxygen atom can be identified as belonging to two or three such octahedra, i.e., as being bonded to either two or three tungsten atoms, on the basis of W–O distance. If the oxidation number of each oxygen atom is −2, then when an oxygen atom is bonded to two tungsten atoms, they will share two units of positive charge, i.e., one unit of positive charge each. Similarly, when an oxygen atom is bonded to three tungsten atoms, each of those atoms can be assigned two-thirds of a unit of positive charge. The oxidation number of a given tungsten atom is obtained by adding up the contributions resulting from each of the oxygen atoms in the distorted octahedron around the tungsten atom. When this is done for $W_{18}O_{49}$ it is found that oxidation numbers of 6, $5\frac{2}{3}$, $5\frac{1}{3}$, and $4\frac{2}{3}$ are present in the ratio 4:6:4:4. The atoms with an oxidation number of 6 occur in the region of the unit cell which has a WO_3-like structure, while those atoms with an oxidation number of $4\frac{2}{3}$ belong to the region which has a WO_2-like structure. The remaining atoms are in the intermediate region. The situation is actually more complicated than this picture suggests, because 2 of the 18 tungsten atoms in the unit cell are separated by a distance similar to the short distance (2.50 Å) between alternate pairs of tungsten atoms in WO_2. These two atoms would be expected to form a bond, as in WO_2, with a smaller chemical shift for the W 4*f* peaks than would otherwise be the case. This reduced chemical shift is observed in the form of a shoulder to lower binding energy on the strongest peak in the W 4*f* spectrum of $W_{18}O_{49}$.

Given the number of different oxidation states in this oxide, the presence of W–W bonding, and the possibility of X-ray induced reduction of the sample (*1*), there is little point in attempting to model the spectrum quantitatively. Nevertheless, the above discussion offers a qualitative explanation for the form of the W 4*f* spectrum of $W_{18}O_{49}$.

Finally, it is of interest to apply the above formalism to $W_{20}O_{58}$. In this case the oxidation numbers are 6, $5\frac{2}{3}$, $5\frac{1}{3}$, and 5 in the ratio 14:2:2:2. In practice, this breakdown is indistinguishable from oxidation numbers of 6 and 5 in the ratio 16:4.

(*b*) *Supported Tungsten Oxides*

The difference in stability of the supported and unsupported tungsten oxides to reduction in both wet and dry hydrogen at high temperatures implies that WO_3 interacts in some way with the alumina support. The nature of this interaction is very sensitive to the particular conditions applied. For example, some authors (*3, 4, 21, 22*) have presented evidence for the formation of $Al_2(WO_4)_3$ in such catalysts, while others (*23–25*) dispute these results. It is expected that at temperatures above 1100°C, substantial bulk $Al_2(WO_4)_3$ formation is possible, but at lower temperatures (e.g., 400°C, as in this work) it is improbable that such a species could be formed, despite the coincidence between the W 4*f* peaks in $Al_2(WO_4)_3$ and the heated 6% WO_3/γ-Al_2O_3.

What are the differences between WO_3 and $Al_2(WO_4)_3$ which give rise to the binding energy variations observed in Fig. 3? The crystal structures of the two compounds may provide insight. As noted previously, the W in WO_3 is octahedrally coordinated to O. $Al_2(WO_4)_3$, however, has quite an open structure (*26*) with the W tetrahedrally coordinated to O and the Al octahedrally coordinated to O. Since a difference in binding energy arises from a difference in the chemical environment, it is reasonable to ascribe the difference in binding energies in the two compounds to the difference in the coordination of the W. Although bulk $Al_2(WO_4)_3$ is almost certainly not formed, it appears that a surface layer of tetrahedrally coordinated W is

formed slowly when the catalyst is heated in air (*24*). Kerkhof *et al.* (*8*) found that WO_3/SiO_2 also comprises reducible and irreducible W. One surface structure which they suggest for the irreducible material has the W tetrahedrally coordinated.

Not surprisingly, it is very difficult to reduce the surface compound in wet hydrogen, although a slight broadening of the feature to lower binding energy of the W $4f_{7/2}$ peak in Fig. 5 can be discerned. Subsequent dry hydrogen treatment did produce a small amount of metal (15%) but this is most likely due to WO_3 being trapped in the pores of the alumina during the impregnation and rising to the surface during calcination and reduction.

If the WO_3/γ-Al_2O_3 sample is calcined in air at very low temperatures very little of the surface material is converted to a tetrahedrally coordinated W compound. This is evidenced by the dry hydrogen reduction of such a sample (Fig. 6), in which most of the WO_3 was quickly reduced to W metal.

Heating 6% WO_3/HT-Al_2O_3 in air also results in the formation of a surface compound which appears to contain tetrahedrally coordinated W. However, there is also some uncharged WO_3 (Fig. 7). This difference between WO_3 supported on γ-Al_2O_3 and HT-Al_2O_3 probably arises from the difference in surface areas. HT-Al_2O_3 has less surface area for interaction with WO_3, some of which remains unreacted and, because it is a semiconductor, uncharged. The presence of unreacted WO_3 on the surface of the HT-Al_2O_3 catalyst may explain why it is a better catalyst than γ-Al_2O_3-supported WO_3.

Heating uncalcined WO_3/HT-Al_2O_3 in wet hydrogen produces large amounts of irreducible material (Fig. 8). The W 4*f* spectrum is very broad, but no uncharged material is present. The positions of the W 4*f* peaks appear to be midway between those observed for uncalcined and calcined samples, suggesting that the surface species formed is not the same as that formed by calcining in air. Dry hydrogen treatment of this sample resulted in a considerable improvement in peak shape for the remaining unreduced component of the spectrum. This fact suggests that the reduced component has arisen from unreacted, but charged, WO_3. This species would appear at a different position from that of the irreducible charged material and would have the effect of broadening the spectrum. This reduced species gives the sample a light blue–grey colour. This is most likely to be an oxygen-deficient species of the $W_{20}O_{58}$ type, although a definite stoichiometry cannot be determined. Because of the difficulty of reducing the surface reacted material, it must be the partially reduced species which catalyses the alkene isomerisation. This conjecture is consistent with the behaviour of the unsupported oxide $W_{20}O_{58}$ which also acts as a catalyst but which is rapidly exhausted. The supported oxide is much more stable to degradation in the alkene stream. The most likely reason for this stability is that the tungsten in the oxide is still octahedrally coordinated but interacts weakly with the alumina. Such an interaction with the surface is in accord with the absence of uncharged material in this sample.

As a result of previous (unpublished) work in this laboratory we believe that the basic sites in the alumina (particularly the HT-Al_2O_3) are the most likely foundations for the formation of irreducible tungsten compounds. The γ-Al_2O_3 used in this study contains about 0.22% sodium before any treatment is applied. On conversion to HT-Al_2O_3 this sodium appears to rise to the surface, thus providing the basic sites necessary for $Al_2(WO_4)_3$ or other tungsten complexes to be formed. Washing the HT-Al_2O_3 with water removes a substantial amount of the sodium, and a sample of 6% WO_3 on this washed alumina yielded more than 40% metal after treatment in wet and dry hydrogen. This result supports the contention that sodium impurities have an effect on the production of irreducible tungsten surface species. However, there is another potential source of sodium impurities. The cata-

lysts are made by impregnation of the alumina with sodium tungstate. This would explain why γ-Al_2O_3-supported WO_3 forms irreducible tungsten species upon heating and why washing the HT-Al_2O_3 does not completely inhibit the formation of irreducible tungsten species upon heating.

The ion scattering results give information about the outermost surface layer. The previous ISS study by Salvati *et al.* (*25*) showed how sensitive this technique is in detecting surface atoms, as opposed to those from the bulk. For increasing loadings of WO_3 the Al is effectively shadowed. With a 24% WO_3 loading (i.e., a monolayer coverage on γ-Al_2O_3) the peak due to Al could no longer be seen. Because our HT-Al_2O_3 has a surface area which is only about 10% of that of the γ-Al_2O_3 used by Salvati *et al.*, our 6% loading should correspond to more than a monolayer. This seems to be confirmed by our XPS results (the presence of uncharged WO_3 on the surface), but the existence of a peak due to Al in the ion scattering spectrum of both uncalcined and calcined 6% WO_3/HT-Al_2O_3 (Fig. 9, curves (c) and (d)) suggests that the WO_3 may not be evenly distributed on the surface of the alumina. The change in W : Al ratio of 0.57 to 4.3 upon calcination confirms that WO_3 rises from pores in the alumina to the surface during calcination. Note that both curve (c) and curve (d) have lower Al peaks than curve (e), supporting the conclusion that little, if any, bulk $Al_2(WO_4)_3$ is formed on the surface by calcination at 400°C.

CONCLUSION

This study has sought to understand the X-ray photoelectron spectra of the four common tungsten oxides and to shed light upon the nature of the surface species on alumina-supported tungsten oxide catalysts. The results for the unsupported tungsten oxides differ somewhat from those of a previous study by de Angelis and Schiavello (*1*), but can be qualitatively understood.

This study has also demonstrated, in agreement with earlier work (*3, 4, 21, 22*), that WO_3 interacts with the alumina support when heated at 400°C or above. Sodium impurities in the alumina and from catalyst impregnation assist in this process, which occurs for both γ-Al_2O_3 and HT-Al_2O_3, although the smaller surface area of the latter results in some free WO_3 remaining on the surface. The surface species formed by the interaction between WO_3 and Al_2O_3 is not $Al_2(WO_4)_3$, but has tetrahedrally coordinated W. Possibly because of the method of impregnation, the WO_3 is not uniformly distributed on the surface of the HT-Al_2O_3 catalysts. Calcination causes WO_3 to rise from pores in the alumina to give a more uniform coverage.

Reduction of 6% WO_3/HT-Al_2O_3 in wet hydrogen leads to an irreducible surface species, possibly different from that obtained by calcining in air. Because of the difficulty in reducing the surface compound, it is likely that catalysis takes place on the unreacted, partially reduced WO_3, which is stabilised by a weak interaction with the alumina. We are unable to give a formula for the reduced species. However, from the blue–grey colour of the catalyst after wet hydrogen treatment, we surmise that it is an oxygen-deficient species of the $W_{20}O_{58}$ type.

ACKNOWLEDGMENTS

Valuable discussions with Dr. N. J. Clark and Dr. E. Summerville are gratefully acknowledged. We also thank Dr. E. Summerville for preparing the samples of the supported catalysts.

REFERENCES

1. de Angelis, B. A., and Schiavello, M., *J. Solid State Chem.* **21,** 67 (1977).
2. Haber, J., Stoch, J., and Ungier, L., *J. Solid State Chem.* **19,** 113 (1976).
3. Biloen, P., and Pott, G. T., *J. Catal.* **30,** 169 (1973).
4. Pott, G. T., and Stork, W. H. J., *in* "Preparation of Catalysts" (P. Delmon, P. A. Jacobs, and G. Poncelet, Eds.), p. 532. Elsevier, Amsterdam, 1976.
5. Delgass, W. N., Hughes, T. R., and Fadley, C. W., *Catal. Rev.* **4,** 179 (1970).

6. Baker, B. G., and Clark, N. J., "New Fischer–Tropsch Catalysts." Report of NERDDC Project No. 132, 1983.
7. Baker, B. G., Clark, N. J., Summerville, E., and McArthur, H., "Catalysts." (a) General Patent No. PF5478/82 (1982); (b) International Patent No. PCT/AU83/00110 (1983).
8. Kerkhof, F. P. J. M., Moulijn, J. A., and Heeres, A., *J. Electron Spectrosc. Relat. Phenom.* **14,** 453 (1978).
9. Andreini, A., and Mol, J. C., *J. Colloid Interface Sci.* **84,** 57 (1981).
10. Stork, W. H. J., and Pott, G. T., *Recl. Trav. Chim. Pays-Bas* **96,** 105 (1977).
11. Siem-Sanchez, C., and Kieffer, R., *Rev. Port. Quim.* **19,** 328 (1977).
12. Engelhardt, J., *J. Mol. Catal.* **8,** 161 (1980).
13. Hattori, H., Asada N., and Tanabe, K., *Bull. Chem. Soc. Japan* **51,** 1704 (1978).
14. Soled, S., Murrell, L., Wachs, I., and McVicker, G., *in* "Symposium on the Role of Solid State Chemistry in Catalysts," p. 1310. Washington, DC, 1983.
15. Wells, A. F., "Structural Inorganic Chemistry," 4th ed., p. 457. Oxford Univ. Press, London, 1975.
16. Magneli, A., *Ark. Kemi* **1,** 513 (1950).
17. Sundberg, M., and Tilley, R. J. D., *Phys. Status Solidi A* **22,** 677 (1974).
18. Gmelin Handbuch, Wolfram, *Erg.-Bd. B* **2,** 57 (1979).
19. Wells, A. F., "Structural Inorganic Chemistry," 4th ed., pp. 202, 448. Oxford Univ. Press, London, 1975.
20. Magneli, A., *Ark. Kemi* **1,** 223 (1950).
21. Stork, W. H. J., Collegem, J. G. F., and Pott, G. T., *J. Catal.* **32,** 497 (1974).
22. Tittarelli, P., Iannibello, A., and Villa, P. L., *J. Solid State Chem.* **37,** 95 (1981).
23. Thomas, R., Kerkhof, F. P. J. M., Moulijn, J. A., Medema, J., and de Beer, V. H. J., *J. Catal.* **61,** 559 (1980).
24. Ng, K. T., and Hercules, D. M., *J. Phys. Chem.* **80,** 2094 (1976).
25. Salvati, L., Makovsky, L. E., Stencel, J. M., Brown, F. R., and Hercules, D. M., *J. Phys. Chem.* **85,** 3700 (1983).
26. Craig, D. C., and Stephenson, N. C., *Acta Crystallogr. Sect. B* **24,** 1250 (1968).